



Haplosufficiency of PAX3 for melanoma development in Tyr: NRASQ61K; Cdkn2a-/- mice allows identification and sorting of melanoma cells using a Pax3GFP reporter allele.

Cécile Campagne, Edouard Reyes-Gomez, Sophia Loiodice, Stéphanie Gadin, Jacky Ezagal, Florence Bernex, Marie Abitbol, Anne Louise, Friedrich Beermann, Jean-Jacques Panthier, et al.

► To cite this version:

Cécile Campagne, Edouard Reyes-Gomez, Sophia Loiodice, Stéphanie Gadin, Jacky Ezagal, et al.. Haplosufficiency of PAX3 for melanoma development in Tyr: NRASQ61K; Cdkn2a-/- mice allows identification and sorting of melanoma cells using a Pax3GFP reporter allele.. Melanoma Research, 2016, 26 (1), pp.12-20. 10.1097/CMR.0000000000000212 . pasteur-01329627

HAL Id: pasteur-01329627

<https://pasteur.hal.science/pasteur-01329627>

Submitted on 9 Jun 2016

HAL is a multi-disciplinary open access archive for the deposit and dissemination of scientific research documents, whether they are published or not. The documents may come from teaching and research institutions in France or abroad, or from public or private research centers.

Copyright

L'archive ouverte pluridisciplinaire **HAL**, est destinée au dépôt et à la diffusion de documents scientifiques de niveau recherche, publiés ou non, émanant des établissements d'enseignement et de recherche français ou étrangers, des laboratoires publics ou privés.

Haplosufficiency of PAX3 for melanoma development in *Tyr::NRAS^{Q61K}; Cdkn2a^{-/-}* mice allows identification and sorting of melanoma cells using a *Pax3^{GFP}* reporter allele

Running title: *Pax3^{GFP}* allele and fluorescent melanoma development *in vivo*

Cécile Campagne^{1,2,#,*}, Edouard Reyes-Gomez^{1,2,3}, Sophia Loiodice^{1,2,§}, Stéphanie Gadin^{1,2}, Jacky Ezagal^{1,2}, Florence Bernex^{1,2,3,Ψ}, Marie Abitbol^{1,2}, Anne Louise⁴, Friedrich Beermann⁵, Jean-Jacques Panthier^{1,2,6}, Geneviève Aubin-Houzelstein^{1,2,6} & Giorgia Egidy^{1,2,6,*}.

Affiliations :

1 INRA, UMR955 de Génétique fonctionnelle et médicale, Ecole Nationale Vétérinaire d'Alfort, 7 avenue du Général de Gaulle, Maisons-Alfort, F-94704 France.

2 Université Paris Est, Ecole Nationale Vétérinaire d'Alfort, 7 avenue du Général de Gaulle, Maisons-Alfort, F-94704 France.

3 Université Paris-Est, Ecole Nationale Vétérinaire d'Alfort, Unité d'Embryologie, d'Histologie et d'Anatomie pathologique, 7 avenue de Général de Gaulle, Maisons-Alfort, F-94704 France.

4 Plate-forme de Cytométrie, Département d'Immunologie, Institut Pasteur, Paris, France

5 ISREC, Ecole Polytechnique Fédérale de Lausanne, CH-1015 Lausanne, Switzerland.

6 Institut Pasteur, Unité de Génétique Fonctionnelle de la Souris; CNRS URA 2578, Département de Biologie du Développement, USC INRA, 25 rue du Dr. Roux, Paris, F-75724 France.

Current addresses: # Department of Radiation Oncology, Memorial Sloan-Kettering Cancer Center, New York 10065, NY, USA; § CRC – UMRS 872, 15 rue de l'Ecole de Médecine, Paris 393 F-75006, France. Ψ Current address: RHEM- Réseau d'Histologie Expérimentale de Montpellier. IRCM Institut de Recherche en Cancérologie de Montpellier, INSERM U1194, Montpellier, F-34298, France.

***Corresponding authors:** Giorgia Egidy; INRA, UMR955 de Génétique fonctionnelle et médicale, Ecole Nationale Vétérinaire d'Alfort, 7 avenue du Général de Gaulle, Maisons-Alfort, F-94704 France; e-mail: gegidy@jouy.inra.fr; tel: +33 (0)1 3465 2128; fax: +33 143 967 169. Cécile Campagne: Department of Radiation Oncology, Memorial Sloan-Kettering Cancer Center, New York 10065, NY, USA; e-mail: campagnc@mskcc.org

Source of fundings: This work was supported by grants from the Institut National de la Recherche Agronomique, the Agence Nationale de la Recherche Emergence Bio and the Association pour la Recherche contre le Cancer. CC was granted by Allocation de Recherche MENRT from the French Ministry of Research.

Conflict of interests: none declared.

"This is a non-final version of an article published in final form in (provide complete journal citation)".

Abstract

The role of the *Pax3* gene in embryonic development of pigment cells is well characterized. By contrast, the function of *Pax3* in melanoma development is controversial. Indeed, data obtained from cultured cells suggest that PAX3 may contribute to melanomagenesis, and PAX3 is found overexpressed in melanomas but also in nevi compared to normal skin samples. *Pax3* homozygous loss of function is embryonic lethal. In order to assess the role of *Pax3* in melanoma development *in vivo*, we analyzed *Pax3* haploinsufficiency in a mouse model of melanoma predisposition.

The *Pax3*^{GFP/+} knock-in reporter system was combined with the *Tyr::NRAS*^{Q61K}; *Cdkn2a*^{-/-} mouse melanoma model. Melanoma development was followed over 18 months. Histopathological, immunohistochemical and molecular analyses of lesions at different stages of melanoma progression were performed. Fluorescence-activated cell sorting on GFP of cells from primary or metastatic melanoma was followed by *ex vivo* transformation tests and *in vivo* passaging.

We report here that *Tyr::NRAS*^{Q61K}; *Cdkn2a*^{-/-}; *Pax3*^{GFP/+} mice developed metastasizing melanoma as their *Tyr::NRAS*^{Q61K}; *Cdkn2a*^{-/-} littermates. Histopathology revealed no differences between the two genotypes, although *Pax3* mRNA and PAX3 protein levels in *Pax3*^{GFP/+} lesions were reduced by half. *Pax3*^{GFP} allele proved a convenient marker to identify and directly sort heterogeneous populations of melanoma cells within the tumor bulk at each stage of melanoma progression.

This new mouse model represents an accurate and reproducible means for identifying melanoma cells *in vivo* to study mechanisms of melanoma development.

Key words: PAX3, mouse melanoma models, primary culture, direct FACS-sorting, immunohistology.

Introduction

The Paired box 3 (PAX3) transcription factor is a key regulator of pigment cells development during embryogenesis [1]. *Pax3* gene is expressed in melanoblasts and melanocytes. Several pieces of evidence suggest that *Pax3* may be involved in the formation of melanomas. *Pax3* is expressed by neoplastic melanocytes in nevi and melanomas [2]. PAX3 transcription factor was shown to modulate mRNA expression levels of genes known to be involved in differentiation, proliferation and survival of melanoma cultured cells [3]. In addition, silencing *Pax3* using RNA interference was shown to inhibit proliferation, and induce terminal differentiation and apoptosis following activation of caspase-3 and p53 in melanoma cells [4-6]. More recently, *Pax3* silencing was reported to inhibit invasiveness of melanoma cells in culture [7] as well as the growth of melanoma cells with acquired resistance to vemurafenib [8]. PAX3 is also expressed in muscle progenitor cells before myogenic transcription factors, such as MyoD, Myogenin, and Myf5 and gradually declines during muscle differentiation. Interestingly, human *PAX3* gene is re-expressed in some cancers such as rhabdomyosarcomas and Ewing's sarcoma, suggesting that PAX3 may play a role in human malignancies [9]. To test the role of *Pax3* in melanocyte transformation to melanoma, we analyzed the effect of haploinsufficiency for *Pax3* in a model of cutaneous metastasizing melanoma. We took advantage of *Tyr::NRAS^{Q61K}*; *Cdkn2a*^{-/-} mice that carry a transgene for a dominant-active NRAS targeted to the melanocyte lineage by the *Tyrosinase* promoter (*Tyr*) and a deletion at the *Cdkn2a* locus which encodes the two tumor suppressor proteins p16^{INK4A} and p14^{ARF}. These mice develop pigmented melanomas that acquire the ability to metastasize [10]. We have recently proposed a histopathological classification for melanocytic lesions in this model [11]. *Tyr::NRAS^{Q61K}*; *Cdkn2a*^{-/-} mice were mated with *Pax3*^{GFP/+} mice. In *Pax3*^{GFP/+} mice, the reporter gene *GFP* is inserted into the first exon of the *Pax3* gene, leading to a null allele with GFP expression in PAX3-positive cells [12]. Our hypothesis was that

reduced *Pax3* expression in *Pax3*^{GFP/+} mice, compared to *Pax3*^{+/+} homozygous mice, would delay melanocyte transformation to melanoma in *Tyr::NRAS*^{Q61K}; *Cdkn2a*^{-/-} mice, thus slowing down the metastatic process. To our surprise, *Tyr::NRAS*^{Q61K}; *Cdkn2a*^{-/-}; *Pax3*^{GFP/+} mice developed cutaneous metastasizing melanoma with clinical features similar to the ones of their *Tyr::NRAS*^{Q61K}; *Cdkn2a*^{-/-}; *Pax3*^{+/+} littermates. We further tested whether the *Pax3*^{GFP} allele could be used as a convenient marker to identify and sort melanoma cells within the tumor bulk. Primary cultures of melanocytic cells, from non-transformed melanocyte to melanoma cells of various stages of progression, were obtained. Sorted cells kept specific essential attributes of their stage of origin. Therefore the *Pax3*^{GFP} allele provides a usable marker for melanoma cells in the mouse.

Methods

Mice and genotyping. Transgenic *Tyr::NRAS*^{Q61K} were produced at the Swiss Institute for Experimental Cancer Research [10]; *Cdkn2a*^{-/-} at the Albert Einstein College of Medicine [13] and *Pax3*^{GFP/+} mice at the Institut Pasteur [12]. These three mouse lines have been backcrossed onto the C57BL/6J background for more than 15 generations. Eight week-old C57BL/6J females were used for intra-venous injection of 10⁶ syngeneic tumoral cells. (agreement n° 16 notice 14/02/12-4). Details on mice genotyping can be found in supplementary material.

Histologic analysis and immunofluorescence in mouse samples. Complete necropsy, systematic histopathological analysis with routine hematoxylin-eosin-saffron (HES) staining and classification of melanocytic lesions were performed on *Tyr::NRAS*^{Q61K}; *Cdkn2a*^{-/-}; *Pax3*^{GFP/+} (N=33), and *Tyr::NRAS*^{Q61K}; *Cdkn2a*^{-/-}; *Pax3*^{+/+} (N=65) adult mice, as described [14]. Briefly, grossly not remarkable cutaneous pigmented lesions with benign features were classified as nevi. Microscopically, they consisted of dermal stellate shaped and heavily

pigmented melanocytes in the vicinity of hair follicles. Early nevi were composed of melanocytes with small nuclei separated by collagen bundles. Late nevi had higher cellular density, fewer collagen bundles and displayed larger yet bland nuclei. Grossly visible nodules forming plaques <2mm were identified as atypical nevi. These lesions were ill demarcated and exhibited features suggestive of malignancy like moderate to low nuclear-cytoplasmic ratio (NCR), larger nucleoli, pleomorphism and rare mitoses. Cutaneous melanomas were usually larger than 2mm. Melanomas were located in the dermis and hypodermis. They displayed (i) high cellular density, (ii) frank nuclear atypias, (iii) increased number of mitosis and (iv) usually low pigmentation. Necrosis was common. Lung metastases were multifocal and composed of variably pigmented and pleomorphic cells arranged around vessels [14]. Direct fluorescence was detected in frozen sections with DAPI counterstaining upon overnight fixation in 0.5% paraformaldehyde in 4% sucrose of skin and lung. For immunofluorescence analyses, antigen retrieval was performed in citrate buffer pH 6 for 30 min in a water-bath. Blocking was performed for 1h at RT in 10% normal goat serum, bovine serum albumin 1% in PBS. Primary antibodies (list in supplementary material) were incubated overnight at 4°C. Secondary Alexa-fluor antibodies (Invitrogen, 1:400) were incubated for 1h at RT, with Alexa-fluor 488 reserved exclusively for the anti-GFP antibody as endogenous GFP was not completely lost with fixation. The sections were then mounted in Vectashield (Vector, Abcys, Courtaboeuf, France). Sections were examined with a Zeiss Axio Observer Z1M ApoTome microscope (Carl Zeiss S.A.S.; Le Pecq, France). Images were processed with the *AxioVision* computer program version 4.6 (Carl Zeiss) and colors could be changed. Figures are representative of the skin samples evaluated (N>8 for each line). All images are individual sections of z series stack. Final figures were assembled with Adobe Photoshop CS6 (Adobe Systems; USA).

RNA extraction and RT-qPCR. RNA extractions were performed on formalin-fixed, paraffin-embedded (FFPE) melanoma samples collected from *Tyr::NRAS^{Q61K}*; *Cdkn2a*^{-/-}; *Pax3*^{+/+} (N=5) or *Tyr::NRAS^{Q61K}*; *Cdkn2a*^{-/-}; *Pax3*^{GFP/+} (N=5) mice using NucleoSpin FFPE RNA kit (Macherey-Nagel, Hoerd, France). Reverse transcriptions were performed using Maxima First Strand cDNA Synthesis kit (Fermentas, Thermo fisher, Villebon s/Yvette, France). qPCR were performed using Maxima SYBR green qPCR kit (Fermentas) on a Roche Light Cycler Carousel-based system (Roche). All methods followed manufacturer's instructions qPCR primers are available in supplementary material. qPCR experiments were carried out at least twice in triplicates.

Protein extractions and western-blot analyses. Before loading on 10% acrylamide gels, proteins were denatured 5 min at 95°C. Transfer was realized on PVDF membrane. The primary antibodies were rabbit anti-PAX3 (Zymed, Invitrogen, 1:1000, Cergy Pontoise, France,) and mouse anti- α -tubulin (eBioscience, 1:2000, Paris, France). Quantification was made using ImageJ software.

Fluorescent activated cell sorting (FACS). FACS-sorting of melanocytes was performed as previously described [15]. Primary cutaneous melanomas and metastases from lymph nodes or lungs sampled at necropsy were finely chopped and incubated for 20 min at 37°C under agitation in collagenase type IV (Gibco Invitrogen Cell Culture, Cergy Pontoise, France), liberase TM (Roche, Meylan, France) and DNase (Epicentre, Tebu-bio, Le Perray, France). Supernatant was neutralized in DMEM medium containing 10% FCS and remaining tissues were incubated in a new digestion mix for 10 additional minutes. Cell suspensions were filtered, centrifuged and resuspended in PBS, 2mM EDTA. All acquisitions and data analyses were performed with a MoFlo XDP Flow Cytometer (Beckman Coulter, Villepinte, France) interfaced to FlowJo software. Cells were gated for single events and viability, then sorted on GFP expression. Three to six samples were FACS-sorted for each stage of melanoma.

Cell culture and immunofluorescence. FACS-sorted melanocytes were cultured without feeder cells as described [15]. Experiments herein used cells trypsinized up to 5 passages. For immunofluorescence, cells were plated onto cover slips for 24 h, then fixed 15 min with 2% paraformaldehyde, permeabilized 10 min with ice-cooled methanol and labeled as described above.

Soft agar Assay. Approximately 5×10^4 cells/ mL and 5×10^5 cells/ mL were seeded in quintuplicates in 96-well plates with Seaplaque agar, and observed 12 days later. The assay was performed twice.

Modified Boyden chamber assay. Approximately 2×10^4 cells were placed onto Matrigel coated cell culture inserts (0.8 μM pore, R&D-Systems) in quintuplicates. These inserts were suspended over 24-well plates containing DMEM and 1% FCS, as chemoattractant. Twenty four hours later, the cells on the underside of insert filters were fixed, stained with cresyl violet and counted under a bright-field microscope. The assay was performed twice.

Statistical analysis. All error bars in the figures represent standard error of the mean. Student's t-test or nonparametric Mann-Whitney U test were used to assess differences between groups. A *P*-value <0.05 was considered as statistically significant.

Results

Generation of *Tyr::NRAS^{Q61K}*; *Cdkn2a*^{-/-}; *Pax3*^{GFP/+} mice

Pax3^{GFP/+} mice exhibit a coat color characterized by a variably-sized white belly spot, with white tail tip and paws reflecting defective migration of melanoblasts during embryogenesis (Fig. 1a), as observed in heterozygous *Splotch* (*Pax3*^{Sp/+}) mice [16]. We mated *Pax3*^{GFP/+} knock-in mice with *Tyr::NRAS^{Q61K}*; *Cdkn2a*^{-/-} mice that exhibit skin hyperpigmentation (Fig. 1b). *Tyr::NRAS^{Q61K}*; *Cdkn2a*^{-/-}; *Pax3*^{GFP/+} mice exhibited a compound phenotype with skin

hyperpigmentation due to transgenic $N\text{-}RAS}^{Q61K}$ expression, and a white belly spot and white paws caused by *Pax3* haploinsufficiency (Fig. 1c).

Melanoma development in *Tyr::NRAS}^{Q61K}*; *Cdkn2a}^{-/-}*; *Pax3}^{GFP/+}* mice

Mice were examined for melanocytic cutaneous lesions. All mice developed the spectrum of dermal melanocytic proliferation previously identified in *Tyr::NRAS}^{Q61K}*; *Cdkn2a}^{-/-}*; *Pax3}^{+/+}* individuals [14]. Grossly visible nodules and plaques (<2mm) could be observed in 80% of the animals of both genotypes (Fig 2a). Twenty two out of 65 *Tyr::NRAS}^{Q61K}*; *Cdkn2a}^{-/-}*; *Pax3}^{+/+}* control mice presented cutaneous nodules larger than 2mm wide compared to 11 out of 33 *Tyr::NRAS}^{Q61K}*; *Cdkn2a}^{-/-}*; *Pax3}^{GFP/+}* mice (Fig. 2b). Focal and distant metastases were detected upon complete necropsy in mice with both genotypes (Fig. 2c, d). The incidence of lung metastases was similar in both genotypes: 7 out of 22 control mice, and 4 out of 11 *Tyr::NRAS}^{Q61K}*; *Cdkn2a}^{-/-}*; *Pax3}^{GFP/+}* mice developed lung metastasis (Student's t test; $P>0,05$). Systematic histopathological analysis was performed on melanocytic lesions from littermates with both genotypes with criteria summarized in the Methods section. Figure 2 e-g shows representative fields of nevi (Fig. 2e) melanomas (Fig. 2f) and lung metastases (Fig. 2g) which did not differ between both genotypes. No differences in melanoma clinical features – color, size and sites – were identified. No significant differences in either latency or incidence (Mann-Whitney test; $P>0,05$) were seen between the two genotypes over 18 months (Fig. 2h). To summarize, clinical and histopathological features of the *Tyr::NRAS}^{Q61K}*; *Cdkn2a}^{-/-}* melanoma model were independent of *Pax3* gene dosage.

Since clinical characteristics were alike in both genotypes, we investigated the oncogenic driving molecular pathway of the model. $NRAS}^{Q61K}$ causes constitutive activation of the NRAS protein leading to extracellular signal-regulated kinase (ERK) activation. Phospho-ERK signal was detected in melanomas from *Tyr::NRAS}^{Q61K}*; *Cdkn2a}^{-/-}*; *Pax3}^{GFP/+}* and control mice. This suggests that the ERK pathway was not altered in *Pax3}^{GFP/+}* transformed

melanocytes (Fig. S1). To further explore if PAX3 was necessarily increased in melanomas, we tested whether melanoma lesions had developed by upregulation of the *Pax3* wild type allele. *Pax3* mRNA and PAX3 protein levels were evaluated in primary melanomas from *Tyr::NRAS^{Q61K}*; *Cdkn2a*^{-/-}; *Pax3*^{GFP/+} and control mice. Quantification confirmed a reduction by half of the amounts of *Pax3* mRNA and PAX3 protein in melanomas from *Tyr::NRAS^{Q61K}*; *Cdkn2a*^{-/-}; *Pax3*^{GFP/+} mice compared with the controls (Student's t test; $P<0.05$; Fig. 2i, j). These data indicate that no compensation from the wild type allele took place in *Tyr::NRAS^{Q61K}*; *Cdkn2a*^{-/-}; *Pax3*^{GFP/+} mice melanomas. Altogether, *Pax3* appears to be haplosufficient for melanoma development in the *Tyr::NRAS^{Q61K}*; *Cdkn2a*^{-/-} model.

***Pax3*^{GFP} allele and melanoma cells sorting by FACS**

We have recently shown that the *Pax3*^{GFP} allele provides a valuable reporter to identify melanocytes and their precursors in hair follicle biopsies based on GFP expression [15]. We used the direct fluorescence of GFP expression in melanomas from *Tyr::NRAS^{Q61K}*; *Cdkn2a*^{-/-}; *Pax3*^{GFP/+} mice to identify transformed melanocytes. The GFP signal was strong in the nucleus, and fainter in the cytoplasm of melanoma cells (Fig. 3b) as in melanocytes (Fig. 3a). In melanoma sections, PAX3 and GFP colocalized in the same cells by immunofluorescence (Fig. 3c, d).

To obtain pure primary cultures of melanoma cells, primary melanoma (PM), locoregional metastasis (LRMet), and distant metastasis (DMet) were removed from *Tyr::NRAS^{Q61K}*; *Cdkn2a*^{-/-}; *Pax3*^{GFP/+} mice, the tumoral cells were dissociated and melanocytic cells were FACS-sorted on GFP expression. As controls, primary cultures of FACS-sorted melanocytes were isolated from the back skin of pups. Melanoma primary cultures were morphologically diversified, reflecting the heterogeneity of melanoma cells in tumor bulks (Fig. 4a). Cells were variably pigmented. Constitutive ERK activation was detected in all cells of primary

cultures from *Tyr::NRAS^{Q61K}*; *Cdkn2a*^{-/-}; *Pax3*^{GFP/+} mice (Fig. S2) indicating that *Pax3*^{GFP/+} cells were melanocytic cells as they expressed the *Tyr::NRAS^{Q61K}* transgene.

Functional characterization of FACS-sorted melanoma cells

In order to determine if the isolation technique of melanoma cells from the *Tyr::NRAS^{Q61K}* *Cdkn2a*^{-/-}; *Pax3*^{GFP/+} model during the metastatic process was accurate, primary cultures established from PM, LRMet, and DMet tissues were analyzed in detail. Their transformed properties were evaluated both *in vitro* and *in vivo*. Whereas control primary cultures of melanocytes from neonatal skin did not proliferate in soft agar, FACS-sorted melanocytic cells from all tested tumors resulted in colonies within 12 days indicating anchorage-independent proliferation (Fig. 4b). Cell migration and invasion was measured using a modified Boyden chamber assay. FACS-sorted melanocytic cells originating from the tumors were able to migrate by contrast with melanocytes from healthy skin (Student's t test; p<0.05, Fig. 4c). So far, the *in vitro* tests could distinguish only control non-transformed melanocytic cells from the transformed ones. To test their invasive capacities *in vivo*, FACS-sorted melanocytic cells from PM, LRMet, and DMet tissues were retro-orbitaly injected to syngeneic C57BL/6J mice. Two weeks later, the injected mice were euthanized and their lungs were examined. Pigmented nodules were visible in lungs from mice receiving DMet cells. The entire lungs were sliced and observed under the microscope. Some micrometastasis were pigmented but all of them were PAX3 positive and GFP-positive. GFP-positive micrometastases were found in 1 out of 3 C57BL/6J mice injected with PM cells and in 4 out of 4 C57BL/6J mice injected with either LRMet or DMet cells (Figure 4d). Thus primary melanoma cells could be effectively distinguished from more aggressive metastatic melanoma cells. All in all, the *Pax3*^{GFP} allele was useful to sort melanocytic cells from cutaneous tumors and metastasis.

Discussion

Cell lineage fluorescent reporters have proved useful to visualize cells in the mouse under different physiopathological conditions (<http://www.gensat.org/index.html>). The *Pax3*^{GFP} allele provides a valuable fluorescent reporter to identify melanocytic cells in skin biopsies [15]. To test whether it is also a valuable marker of melanocytic cells in tumors, *Tyr::NRAS*^{Q61K}; *Cdkn2a*^{-/-} and *Pax3*^{GFP/+} mice were bred to produce compound mutant mice. The hyperpigmentation/white bellied phenotype of the triple mutants suggests an absence of genetic interaction between *Pax3* and *Tyr* gene regulation. Noteworthy, *Pax3* transcripts are first detected at day 8.5 in the embryo in the dorsal-most cells of the neuroepithelium [17], whereas the *Tyr* gene is expressed at later stages around midgestation [18]. PAX3 is not known to participate in the regulation of *Tyr* transcription either directly [19] or indirectly [4]. Considering the reports on PAX3 involvement in the proliferation, migration and invasiveness of melanocytes from pigmented tumors *in vitro*, we expected modifications of melanomagenesis parameters in the *Tyr::NRAS*^{Q61K}; *Cdkn2a*^{-/-} model [14]. However, neither clinical nor histological changes were detected in the tumors of *Tyr::NRAS*^{Q61K}; *Cdkn2a*^{-/-}; *Pax3*^{GFP/+} mice compared to their *Pax3*^{+/+} littermates. These results infirm the hypothesis of an effect of PAX3 levels in the differentiation of melanoma cells. Comparable metastatic rate suggests no overall change in cell migration upon removing one functional copy of *Pax3* gene, implying that *Pax3* is haplosufficient for tumor development. Alternatively, PAX3 could have a stimulatory effect on melanoma through a MDM2-mediated ubiquitination of p53 as shown in mouse embryonic stem cells induced to form neuronal precursors [20]. In that case, the present model with *Cdkn2a* locus inactivation would not reveal such interactions. However, melanoma development in *Cdkn2a*^{+/+} mice did not show clinical differences either (data not shown).

Yet some reports seem to be in accordance with our results. In fact, complex regulation of PAX3 transcriptional activities have been described which could explain a lack of phenotype of *Pax3*^{GFP/+} on melanoma initiation, progression and metastasis. First, the histone deacetylase HDAC10 has been shown to relieve repression of PAX3 on *MITF*, *TRP-1* and *DCT* promoters [21] suggesting that deacetylation of PAX3 could be an additional layer of melanomagenesis regulation. Second, Bonvin *et al.* have shown that PAX3 is an activator of *BRN2* expression, which is considered to be a regulator of melanomagenesis. However the range of PAX3 reduction obtained herein could still not affect BRN2 levels which were shown not to be particularly sensitive to PAX3 levels [7]. Third, interestingly enough, in human melanoma cell lines, levels of PAX3 and MITF were found to vary from 15 to 100 fold [22] suggesting that transformation is not dependent on these levels. Fourth, only 60% of human melanoma tissue samples showed *PAX3* expression by *in situ* hybridization [6] accounting for an inter-individual variation in *PAX3* expression which, in light of the present data, would confirm PAX3 haplosufficiency for melanomagenesis.

Cell isolation from cutaneous and metastatic lesions in *Tyr::NRAS*^{Q61K}; *Cdkn2a*^{-/-}; *Pax3*^{GFP/+} mice and identification of melanocytic cells were particularly efficient when the cells were sorted on GFP expression. Importantly, *Cdkn2a* locus deletion avoided senescence of the primary cultures [23]. At the early passages high cell heterogeneity corresponded probably to the *in vivo* variety of cellular types, including the so called cancer stem cells, within the tumor bulk. This material would be a useful tool for new drug screening with the ease of *in vitro* testing and the accuracy of *in vivo* biological heterogeneity.

Conclusion

All in all, the primary cultures from FACS-sorted GFP-positive cells presented the properties of their tumoral stage of origin. The *Pax3*^{GFP} allele proved to be a sensitive fluorescent reporter of normal and tumoral melanocytic lineage *in vitro* and *in vivo* ([15] and herein).

Altogether the *Tyr::NRAS^{Q61K}*; *Cdkn2a*^{-/-}; *Pax3*^{GFP/+} model allows easy identification of melanocytes and melanoma cells within tissues without interfering with tumor progression. Considering that a single murine melanoma model cannot reflect all types of human disease, and provided that *Pax3* haplosufficiency occurs in other melanoma models, use of the *Pax3*^{GFP} allele will be a helpful and powerful tool to study mechanisms of melanoma development *in vivo* in different genetic contexts.

Acknowledgments

We would like to thank C. Koënen for mice care, and A. Champeix and P. Wattier for histological technical assistance. We thank F. Khayati for technical indications with the modified Boyden chamber assay. The PAX3 antibody developed by C.P. Ordahl, was obtained from the Developmental Studies Hybridoma Bank developed under the auspices of the NICHD and maintained by the University of Iowa, Department of Biological Sciences, USA.

Manuscript word count: 4631 from page 1 to 18 /5000

Number of display items : 4/4

References

1. Lang D, Lu M M, Huang L, Engleka K A, Zhang M, Chu E Y, et al.: Pax3 functions at a nodal point in melanocyte stem cell differentiation. *Nature* 2005, 433:884-887.
2. He S, Yoon H S, Suh B J, Eccles M R: PAX3 Is extensively expressed in benign and malignant tissues of the melanocytic lineage in humans. *J Invest Dermatol* 2010, 130:1465-1468.
3. Medic S, Rizos H, Ziman M: Differential PAX3 functions in normal skin melanocytes and melanoma cells. *Biochem Biophys Res Commun* 2011, 411:832-837.
4. He S, Li C G, Slobbe L, Glover A, Marshall E, Baguley B C, et al.: PAX3 knockdown in metastatic melanoma cell lines does not reduce MITF expression. *Melanoma Res* 2010.
5. He S J, Stevens G, Braithwaite A W, Eccles M R: Transfection of melanoma cells with antisense PAX3 oligonucleotides additively complements cisplatin-induced cytotoxicity. *Mol Cancer Ther* 2005, 4:996-1003.
6. Scholl F A, Kamarashev J, Murmann O V, Geertsen R, Dummer R, Schafer B W: PAX3 is expressed in human melanomas and contributes to tumor cell survival. *Cancer Res* 2001, 61:823-826.
7. Bonvin E, Falletta P, Shaw H, Delmas V, Goding C R: A phosphatidylinositol 3-kinase-Pax3 axis regulates Brn-2 expression in melanoma. *Mol Cell Biol* 2012, 32:4674-4683.
8. Liu F, Cao J, Wu J, Sullivan K, Shen J, Ryu B, et al.: Stat3-targeted therapies overcome the acquired resistance to vemurafenib in melanomas. *J Invest Dermatol* 2013, 133:2041-2049.
9. Wang Q, Fang W H, Krupinski J, Kumar S, Slevin M, Kumar P: Pax genes in embryogenesis and oncogenesis. *J Cell Mol Med* 2008, 12:2281-2294.
10. Ackermann J, Frutschi M, Kaloulis K, McKee T, Trumpp A, Beermann F: Metastasizing melanoma formation caused by expression of activated N-RasQ61K on an INK4a-deficient background. *Cancer Res* 2005, 65:4005-4011.
11. Campagne C, Reyes-Gomez E, Battistella M, Bernex F, Chateau-Joubert S, Huet H, et al.: Histopathological atlas and proposed classification for melanocytic lesions in Tyr::NRas ; Cdkn2a transgenic mice. *Pigment Cell Melanoma Res* 2013.
12. Relaix F, Rocancourt D, Mansouri AB, Buckingham M: A Pax3/Pax7-dependent population of skeletal muscle progenitor cells. *Nature* 2005, 435:948-953.
13. Serrano M, Lee H, Chin L, Cordon-Cardo C, Beach D, DePinho R A: Role of the INK4a locus in tumor suppression and cell mortality. *Cell* 1996, 85:27-37.
14. Campagne C, Reyes-Gomez E, Battistella M, Bernex F, Chateau-Joubert S, Huet H, et al.: Histopathological atlas and proposed classification for melanocytic lesions in Tyr::NRas(Q61K) ; Cdkn2a(-/-) transgenic mice. *Pigment Cell Melanoma Res* 2013, 26:735-742.
15. Djian-Zaouche J, Campagne C, Reyes-Gomez E, Gadin-Czerw S, Bernex F, Louise A, et al.: Pax3(GFP) , a new reporter for the melanocyte lineage, highlights novel aspects of PAX3 expression in the skin. *Pigment Cell Melanoma Res* 2012.
16. Hornyak T J, Hayes D J, Chiu L Y, Ziff E B: Transcription factors in melanocyte development: distinct roles for Pax-3 and Mitf. *Mech Dev* 2001, 101:47-59.
17. Goulding M D, Chalepakis G, Deutsch U, Erselius J, R, Gruss P: Pax-3, a novel murine DNA binding protein expressed during early neurogenesis. *EMBO J* 1991, 10:1135-1147.
18. Loftus S K, Baxter L L, Buac K, Watkins-Chow D E, Larson D M, Pavani W J: Comparison of melanoblast expression patterns identifies distinct classes of genes. *Pigment Cell Melanoma Res* 2009, 22:611-622.
19. Galibert M D, Yavuzer U, Dexter T J, Goding C R: Pax3 and regulation of the melanocyte-specific tyrosinase-related protein-1 promoter. *J Biol Chem* 1999, 274:26894-26900.
20. Wang X D, Morgan S, Cloken M R: Pax3 stimulates p53 ubiquitination and degradation independent of transcription. *PLoS One* 2011, 6:e29379.

21. Lai I L, Lin T P, Yao Y L, Lin C Y, Hsieh M JYang W M: Histone deacetylase 10 relieves repression on the melanogenic program by maintaining the deacetylation status of repressors. *J Biol Chem* 2010, 285:7187-7196.
22. He S, Li C G, Slobbe L, Glover A, Marshall E, Baguley B C, et al.: PAX3 knockdown in metastatic melanoma cell lines does not reduce MITF expression. *Melanoma Res* 2011, 21:24-34.
23. Sviderskaya E V, Hill S P, Evans-Whipp T J, Chin L, Orlow S J, Easty D J, et al.: p16(INK4a) in melanocyte senescence and differentiation. *J Natl Cancer Inst* 2002, 94:446-454.

Figure legends

Figure 1. *Tyr::NRAS^{Q61K}; Cdkn2a^{-/-}; Pax3^{GFP/+}* mice

a-c: Phenotype of (a) *Cdkn2a^{-/-}; Pax3^{GFP/+}* mice presenting a white belly spot, white feet and tail tip (arrows), (b) *Tyr::NRAS^{Q61K}; Cdkn2a^{-/-}; Pax3^{+/+}* littermates with hyperpigmented skin (arrowheads) and (c) *Tyr::NRAS^{Q61K}; Cdkn2a^{-/-}; Pax3^{GFP/+}* littermates harboring a compound phenotype (arrows, arrowheads).

Figure 2. Melanomagenesis in *Tyr::NRAS^{Q61K}; Cdkn2a^{-/-}; Pax3^{GFP/+}* mice

a-d: a *Tyr::NRAS^{Q61K}; Cdkn2a^{-/-}; Pax3^{GFP/+}* mouse with cutaneous nodules identified as atypical nevi (a, white arrow heads), melanoma (b, white arrow), local metastasis in the lymph node (c, white arrow) and lung metastasis (d). Red asterisk (a-c) indicates the *Pax3* haploinsufficiency for coat color. **e-g:** Histological features (HES staining) of melanocytic nevus (e), primary melanoma (f) and lung metastasis (g) in *Tyr::NRAS^{Q61K}; Cdkn2a^{-/-}; Pax3^{+/+}* control (1) and *Tyr::NRAS^{Q61K}; Cdkn2a^{-/-}; Pax3^{GFP/+}* mice (2). Lesions are histologically indistinguishable among groups. Bars: (e) 200µm; (f) 50µm and 5mm (insert); (g) 100µm. **h:** Kaplan-Meier of melanoma-free survival curves in *Tyr::NRAS^{Q61K}; Cdkn2a^{-/-}; Pax3^{GFP/+}* (dashed line) and in control mice (plain line), **i-j:** *Pax3* mRNA (i) and PAX3 protein (j) levels in primary melanomas from *Tyr::NRAS^{Q61K}; Cdkn2a^{-/-}; Pax3^{GFP/+}* (grey) and control mice (black). The ratio of PAX3/α-tubulin shows that tumors with the *Pax3^{GFP/+}* allele develop with half of PAX3 protein levels (1.1 ± 0.08 versus 0.51 ± 0.04).

Figure 3. *Pax3^{GFP}* allele and melanoma cells identification based on GFP

a: ApoTome microscopy analysis of GFP direct fluorescence (green), mostly nuclear (blue) in epidermis (a1, a2) or melanoma sections (b1-b3) of *Tyr::NRAS^{Q61K}; Cdkn2a^{-/-}; Pax3^{GFP/+}* mice. Bar a: 10µm, Bar b: 20µm **c-d:** ApoTome microscopy analysis of double labeling for

PAX3 (1, green) and GFP (2, magenta) in control (c) and *Tyr::NRAS^{Q61K}*; *Cdkn2a*^{-/-}; *Pax3*^{GFP/+} (d) melanoma sections. Nuclear counterstaining in blue. Corresponding bright-field photographs (a2, b3, c5, d5). The PAX3 signal is nuclear whereas the GFP signal is both nuclear and cytoplasmic. Bar: 10μm.

Figure 4. Characterization of FACS-sorted melanoma cells.

a: Primary culture of primary melanoma, loco-regional metastasis and distant metastasis from *Tyr::NRAS^{Q61K}*; *Cdkn2a*^{-/-}; *Pax3*^{GFP/+} mice showing phenotypic and pigmentation heterogeneity in FACS-sorted cells, **b:** Photomicrographs of a soft agar assay of primary cells during melanoma progression, **c:** Photomicrographs of primary culture cells subjected to the modified Boyden chamber assay, cell quantification, **d:** Fluorescent microscopy of lung metastases sections in syngeneic mice 15 days after retro-orbital injection of the type of primary culture cells indicated.

Haplosufficiency of PAX3 for melanoma development in *Tyr::NRAS^{Q61K}*; *Cdkn2a*^{-/-} mice allows identification and sorting of melanoma cells using a *Pax3^{GFP}* reporter allele

Campagne C *et al.*

Supplementary Materials

Mice genotyping

To identify the *Pax3^{GFP}* transgene, the *GFP* sequence was amplified using the following primers: *GFP* forward: 5'-ttgtggcggatcttgaagttcacccatgc-3'; *GFP* reverse: 5'-acatgaaggcagcacgacttcaagtccg-3'. PCR conditions were 30 s at 94°C, 30 s at 57°C, 40 s at 72°C for 35 cycles. *Pax3^{GFP/+}* pups could also be identified by direct detection of fluorescent GFP⁺ cells on the snout. The primers used to identify the *NRAS^{Q61K}* were: *NRAS* forward: 5'-gatvvvaccatagaggatt-3'; *NRAS* reverse: 5'- ctggcgtattcttacc-3'. PCR conditions were 1 min at 94°C, 1 min at 56°C, 1 min at 72°C for 4 cycles; 30s at 94°C, 30s at 56°C, 30s at 72°C for 30 cycles. The hyperpigmented phenotype was observed in *Tyr::NRAS^{Q61K}* pups from the first week onwards. The primers used to identify the *Cdkn2a* locus were: forward 5'- ctatcaggacatagcgttgg-3' and reverse: 5'-agtgagagttggggacagag-3'. PCR conditions were 1min at 94°C, 1 min at 57°C, 1 min at 72°C for 4 cycles; 30s at 94°C, 45s at 57°C, 30s at 72°C for 30 cycles. The primers used to identify the *Cdkn2a* deleted locus were: forward 5'-atgatgatggcaacgttc-3' and reverse: 5'-gttcccagcggcacaaag- 3'. PCR conditions were 1 min at 94°C, 1 min at 58°C, 1 min at 72°C for 4 cycles; 30s at 94°C, 45s at 58°C, 30s at 72°C for 30 cycles. All PCR were completed with a final extension step at 72°C for 10 min.

Primary antibodies used for immunofluorescence in mice samples.

Immunofluorescence was performed with chicken polyclonal anti-GFP (1: 600, Abcam, Paris, France), rabbit polyclonal anti-PAX3 (1:100, Zymed, Invitrogen, Cergy-Pontoise, France), mouse monoclonal anti-PAX3 (1:200, Developmental Studies Hybridoma Bank, Iowa university, Iowa, USA) and rabbit polyclonal anti-pERK (phospho-p42/44 MAPK, 1:100, Cell Signaling, Ozyme, St Quentin, France) antibodies. Nuclear counter-staining was achieved with 4', 6'-diamidino-2-phenylindole (DAPI) (1:1000, Invitrogen). Controls without the first antibodies showed no unspecific labeling.

qPCR primers. qPCR primers were as follows. PAX3: 5'-tggcagttatggacaaagtg-3' and 5'-gtggaggccgaaacagg-3' and housekeeping gene β -actin: 5'-tccacacccgcaccagttc-3' and 5'-gaccattcccaccatcacacc-3', and cyclophilinA: 5'-caaattgtggaccaaaca-3' and 5'-ccatccagccattcagtcttg-3'. qPCR experiments were carried out at least twice in triplicates.

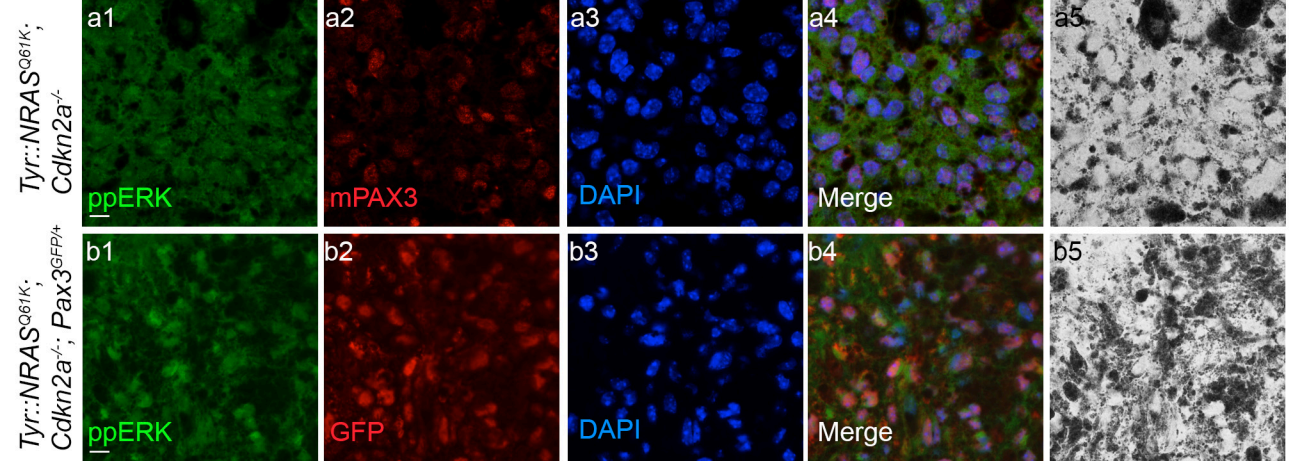
Supplementary Figures

Figure S1. Phospho-ERK staining in melanoma sections.

a-b: ApoTome microscopy analysis of double labeling for pERK (1, green) and Pax3 (a2, red) or GFP (b2, red) in control (a) and *Tyr::NRAS^{Q61K}; Cdkn2a^{-/-}; Pax3^{GFP/+}* (b) melanoma sections. Nuclear counterstaining in blue (3). Corresponding bright-field photographs (5). Bar: 10μm.

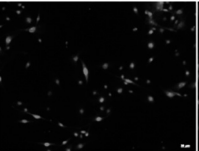
Figure S2. Phospho-ERK staining in FACS-sorted melanocytes and melanoma cells.

ApoTome microscopy analysis of pERK labeling in FACS-sorted melanocytes and melanoma cells at different stages of melanoma progression. Bars: 10μm.

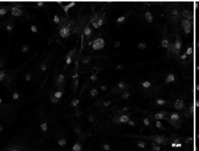


pERK

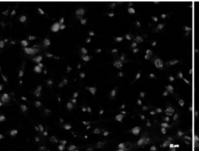
Melanocytes



Primary
melanoma



Loco-regional
metastases



Distant
metastases

